



REINFORCING OF LIQUEFIABLE GROUND USING ANCHORED PLASTIC BOARD DRAIN

Yoshihiro MIZOGUCHI¹, Yasuo TANAKA²

SUMMARY

A laboratory soil test and a numerical simulation were carried out to verify the reinforcing mechanism of ground improvement using a dense array of plastic board drains against ground liquefaction. The laboratory test is to shear a soil element with a group of plastic drains embedded under no volume change condition. The numerical simulation is to employ the discrete element method to examine the reinforcing mechanism of plastic board drains by simulating the above laboratory test. The laboratory test and numerical simulation both show the effectiveness of plastic board drain that prevents the decrease of effective stress in the reinforced soil considerably and therefore would reduce the excess pore pressure built-up considerably.

INTRODUCTION

When liquefaction of ground occurs, heavy damages in various structures are produced as known from the past experiences of earthquakes. The principles of ground improvements for liquefaction countermeasures are the increase of ground density, the increase of effective stress, the dissipation of pore water pressure, and the control of shear deformation, etc. For example, the sand compaction pile method aims the density increase, and the gravel drain method promotes a rapid dissipation of excess pore water pressure. These methods however have high possibilities of causing large vibrations and noises during construction that are disturbing for the existing structures or in urban city. Thus liquefaction countermeasures that have less disturbing effects on existing structures and surroundings are needed and the demands for such methods are increasing since more seismic resistance of urban infrastructures are promoted after the Hyogo-ken Nanbu Earthquake.

A ground improvement method that uses a group of plastic board drains, PBD, has been developed and its advantage is to introduce less construction disturbances to nearby structures. A group of PBD is installed with densely spaced arrays and at the surface the PBD heads are connected by a geo-grid while fixing PBD bottom end anchored to the bearing stratum. The schematic of PBD group installation method is shown in Fig. 1. In this method, a combined effect of reducing the excess pore water pressures and the shear deformation of ground is expected through the drainage and the reinforcing properties, respectively, of PBD and geo-grid.

¹ Asanuma Corporation, Japan, E-mail: mizo@tri.asanuma.co.jp

² Research center for Urban Safety and Security, Kobe University, Japan, E-mail: ytgeotec@kobe-u.ac.jp

The increase of liquefaction resistance by the PBD group installation has been verified through a series of shaking table tests. By reducing the installation spacing of PBD in the group, there was a steady increase of liquefaction resistance of the installed ground, base on the shaking table tests. Although these studies have clearly shown the effectiveness of PBD group installation against liquefaction, the mechanism of liquefaction resistance as a result of PBD installation has not been clarified, and especially the amounts of contributions from the drainage and the reinforcement properties of PBD remained unclear.

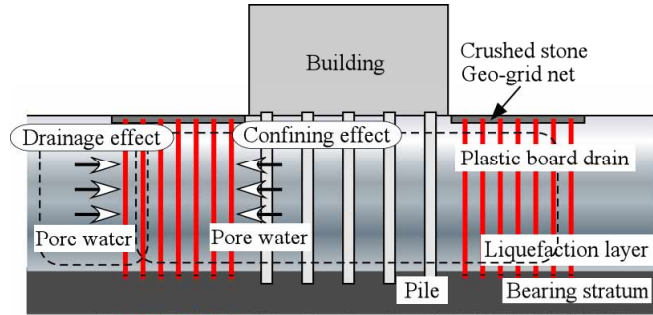


Figure 1: PBD group installation method

Thus, this research was conducted to examine the resistance mechanism of PBD group installation against ground liquefaction. Examination was performed in two steps; first by conducting two different laboratory soil tests on the increased resistance of soil to liquefy with the installation of PBD and then a numerical analysis to examine the reinforcing mechanism of soil with PBD as indicated by the laboratory test. Simple shear soil tests, one in laminated shear box test and the other in torsional hollow cylinder test, were performed with soil specimens with different PBD installations under a constant volume condition. The distinct element method that is suitable for analyzing the interactions between soil particles and PBD was used for analysis. From these laboratory tests and numerical analysis, the influence of the number of PBD, a stiffness of PBD, and a geo-grid related to reinforcing mechanism of soil was investigated. In the numerical analysis above, the drainage effect of PBD was not simulated by assuming only the reinforcing effect.

LABORATORY SOIL TESTS WITH PBD INSTALLATION

Simple shear test on model ground with PBD installation

Test procedure

Photo.1 shows the simple shear test apparatus used for testing model grounds with various PBD installations. The shear box consists of 11 laminated rectangular frames, and the size of shear box is 30cm in length, 20cm in width, and 12 cm in height. The vertical force to the model ground is applied from the bottom by adjusting the air pressure, and the shear force is applied at the top by giving a constant rate of horizontal displacement of screw-gearred piston as shown in the photograph. The height of the shear box was kept constant during the test by adjusting the vertical load on the ground, and this was to simulate the undrained shear of ground. Table 1 and Fig. 2 show the variations of PBD and geo-grid installation arrangements, and altogether five different tests have been performed. In Model 1-5, no PBD was installed in the ground. In Models 1-1 & 1-2, nine PBDs of Type-1 were installed, while in Models 1-3 & 1-4 two PBDs of Type-2 were installed.

The difference between Type-1 and Type-2 of PBD are the strength and the size. Type-1 PBD is made of filter material only, with 10mm in width and 0.8mm in thickness, had a tensile strength of 60N. Type-2 is made of actual PBD material with 20mm in width and 4.4mm in thickness and had a tensile strength of 560N. These PBDs are installed in the model ground with there top tied to a geo-grid net that had much higher tensile strength and stiffness than those of

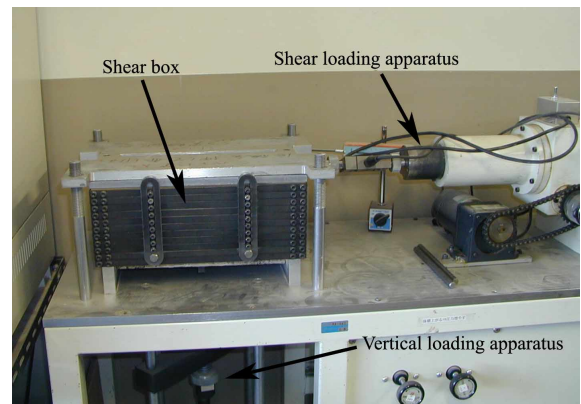


Photo 1: Simple shear test apparatus

Table 1: Case of Simple shear test

Case	Type of PBD	Number of PBD	Upper of PBD	Lower of PBD
Model 1-1	Type-1	3*3=9	Geo-grid net	Geo-grid net
Model 1-2			Geo-grid net	Non-geo-grid net
Model 1-3	Type-2	2*1=2	Geo-grid net	Geo-grid net
Model 1-4			Geo-grid net	Non-geo-grid net
Model 1-5	Non-PBD	0		

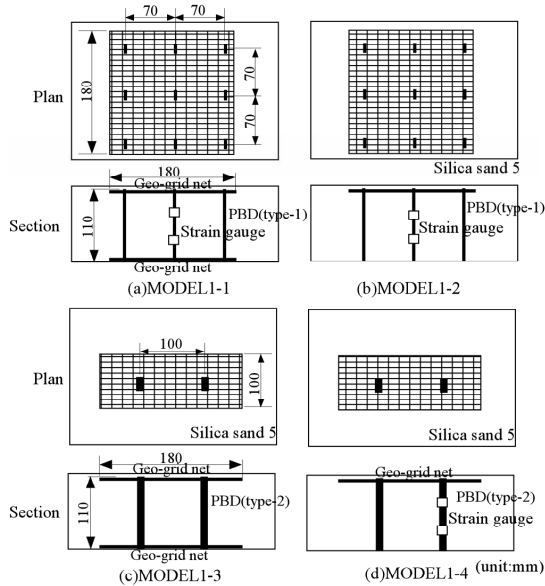


Figure 2: Arrangement of PBD and geo-grid net

PBDs. The bottom ends of PBDs are either tied to the base geo-grid net (Model 1-1 & 1-3), or set free without installing the base geo-grid net (Model 1-2 & 1-4). Silica sand is used to form the model ground, and its gradation curve is shown in Fig.3. The model ground was formed by pulverizing the sand into the shear box in which the PBDs have been pre-installed. The relative density of sand was set to be 50% by adjusting the pulverizing height of sand. The sand ground was consolidated to a vertical stress of 19.6 kN/m², and then sheared at a constant rate of shear strain of 1%/min. During the test, measurements are taken of the horizontal load and displacement, and the vertical load and displacement of shear box at the top. Also the tensile strains of PBD were measured at the positions shown in Fig.2 for three tests (Model 1-1, 1-2, and 1-4).

Test result

The relationship between shear strain and shear stress is shown in Fig. 4 (a). As can be seen from the figure, the shear resistances of all four model grounds with PBD installations becomes larger than that of the ground without PBD for the shear strain greater than 0.3%. As to the differences of geo-grid net installations, the resistance is higher for the PBDs tied to the base geo-grid net (i.e., the resistance is higher for Models 1-1 & 1-3 than Models 1-2 & 1-4 respectively).

The differences among the dilatancy characteristics of model ground are shown in Fig. 4(b), and the decrease of normal stress represents the compressive behavior as the test was performed at a constant

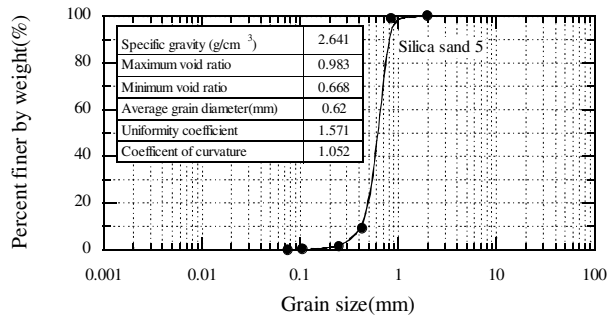


Figure 3: Grading curve

volume (undrained) condition. It is clear that the ground without PBD is the most compressive, and the dilatancy trend increases as the number of installed PBD increases.

Fig. 4(c) shows the effective stress paths of all five model tests. The model ground without PBD (Model 1-5) shows the largest decreases in the effective stress at the start of test, while in other four tests the decreases of effective stress is not so large. As to the difference of geo-grid installations, the resistance is higher for the PBDs with the base geo-grid in comparison with PBDs without the base geo-grid. As to the number of PBD installations, the larger the PBD installation numbers the higher the shear resistance of model ground.

Fig. 5 shows the measured tensile strain of PBDs in Model 1-1 & 1-2 tests. The PBD without the base geo-grid net has rather uniform tensile strains with depth, while the PBD with the base geo-grid has larger concentration of tensile strain near the bottom. Although there is significant difference of tensile strain between these two tests, the depth distribution of tensile strain of PBD may vary considerably depending on where the measured PBD is located as will be discussed later in numerical analysis. There seems to be a considerable non-uniformity in the stress distributions in the model ground for the simple shear testing.

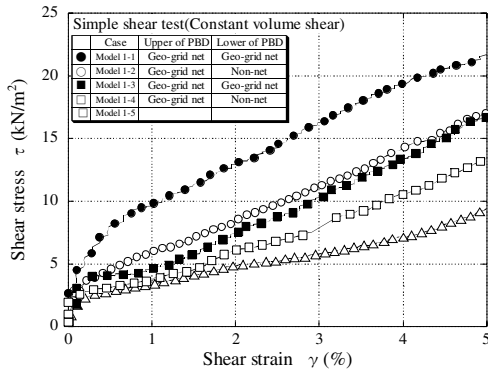


Figure 4(a): Shear stress - shear strain relationship

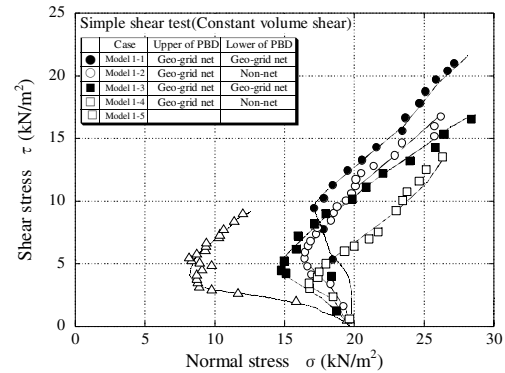


Figure 4(c): Effective stress path

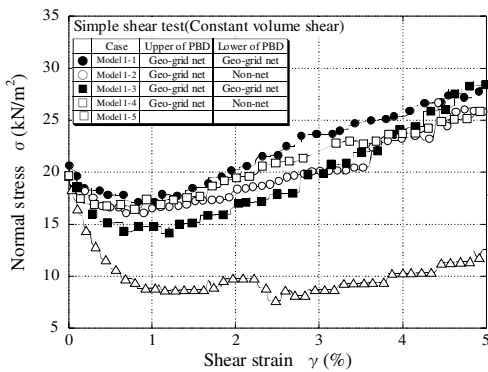


Figure 4(b): Vertical stress - shear strain relationship

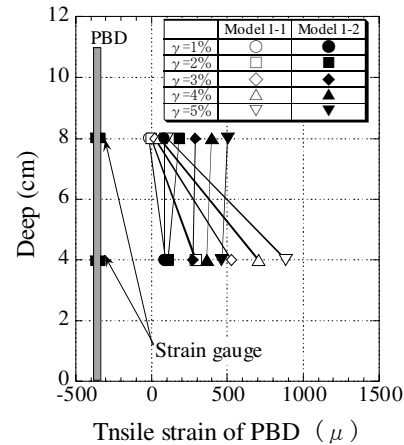


Figure 5: Tension strain of PBD

Torsional shear test on soil element with PBD installation

Test procedure

The test apparatus used for the torsional shear test is shown in Fig. 6. The size of hollow cylindrical specimen has 60mm inner diameter, 100mm outer diameter, and 210mm height. Four tests have been performed as shown in Table 2 by varying the number of PBD installation from 0 to 6. Fig.7 shows the geometry of PBD installations. The upper and lower ends of PBDs are tied to the top cap and pedestal of

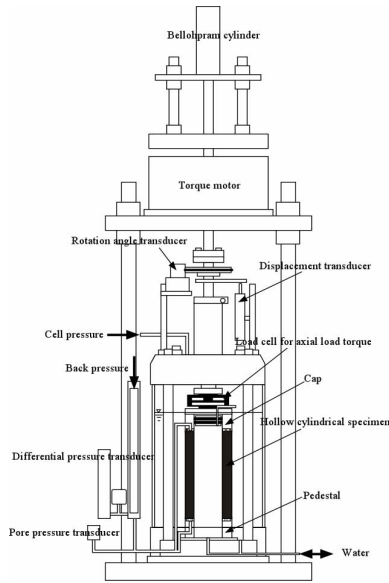


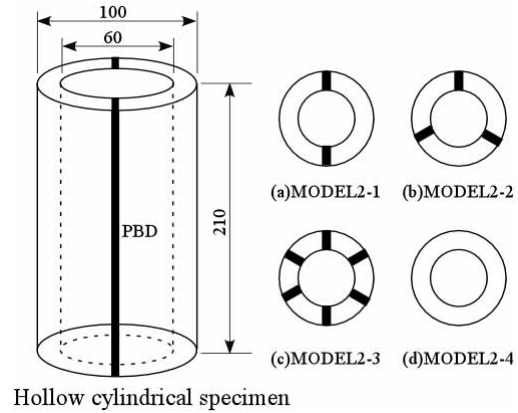
Figure 6: Apparatus of torsional shear test

the apparatus respectively. The same silica sand as previously shown in Fig.3 was used for the test, and the specimen having 50% relative density was prepared by pulverizing the sand into the mold. Type-2 PBD with a width of 10mm was used in the test.

The torsional shear test was performed on saturated specimen while keeping the specimen height constant. By keeping the specimen height constant for saturated specimen, the specimen should deform in plane strain condition that is the same shear deformation condition as imposed for the simple shear testing of model ground. The specimen was sheared under a constant rate of shear strain of 1%/min.

Test result

The relationships between shear strain and shear stress for all four tests are shown in Fig. 8(a). As can be seen from the figure, the shear stiffness becomes larger as the number of PBD installation increases. However, the increasing rate of shear resistance with the shear strain becomes almost the same for all four



Hollow cylindrical specimen

Figure 7: Arrangement of PBD

Table 2: Case of torsional shear test

Case	Number of PBD
Model 2-1	0
Model 2-2	2
Model 2-3	3
Model 2-4	6

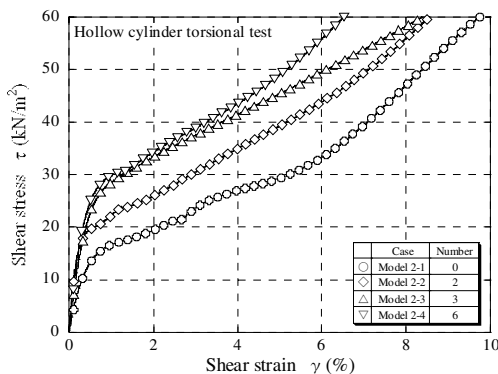


Figure 8(a): Shear stress - shear strain relationship

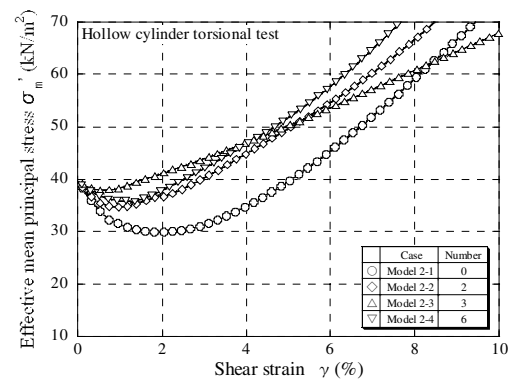


Figure 8(b): Effective mean principal stress - shear strain relationship

tests after the shear strain exceeds 1%. The difference of the dilatancies exhibited by different PBD installations are shown by plotting the changes of effective mean principal stress, σ'_m , with the shear strain in Fig. 8(b). Since the tests have been performed under undrained and constant height conditions, the changes in both the pore water pressure and the vertical stress also indicate the dilatancy characteristics of soil. Thus the changes of effective mean principal stress represent the dilatancy changes of soil with PBD installations. Fig. 8(b) clearly shows that the soil without PBD is most compressive, while the dilatancy increases as the number of PBD installation increases.

The measured effective stress paths during the test are shown in Fig.8 (c), and it shows that the soil without PBD installation exhibits a largest decrease in effective stress with the increase in shear stress. As the number of PBD installation increases, the shear resistance increases accordingly. However, the changes in effective stress during the initial shearing stage of test seems to be nearly the same irrespective of different PBD installations.

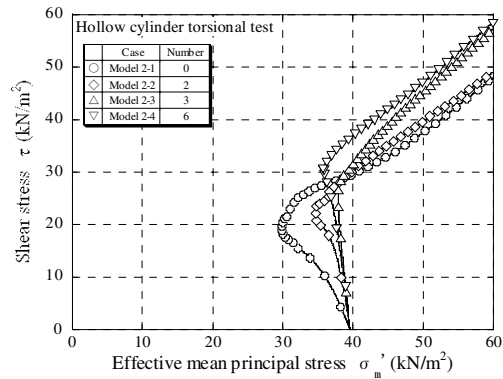


Figure 8(c): Effective stress path

SIMULATION ANALYSIS USING DISTINCT ELEMENT METHOD

Analysis by distinct element method

A distinct element method (it outlines Following DEM) is the numerical analysis technology developed by Cundall (1971). DEM modeled the polygon, and the ball or cylinder form called distinct element as rigid body. The algorithm at the time of asking for the action of this aggregate is very simple. The contact judging with other elements is performed for every element. It asks for contact force by assuming spring or dash pot between particles. The equation of motion obtained from the contact force is solved by time integration.

The flow of DEM used for analysis is shown in Fig. 9. The contact judging of element, the calculation of interaction force, the calculation of the pore water pressure, and calculation of acceleration or velocity or displacement of element are performed repeatedly. In case the liquefaction is treated, it is necessary to evaluate the pore water pressure appropriately. DEM asks each time step for the shrinkage of the pore water by movement of particle and the dissipation of the excess pore water pressure. This time, the analysis method which Fujitani, Nakase and others used was used. The analysis model divides into the mesh, and the increment of the water pressure ask the increment of the pore area in the mesh. The calculation of generating of the excess pore water pressure by particle movement, the calculation of dissipation of the excess pore water pressure by permeability, and the calculation of the

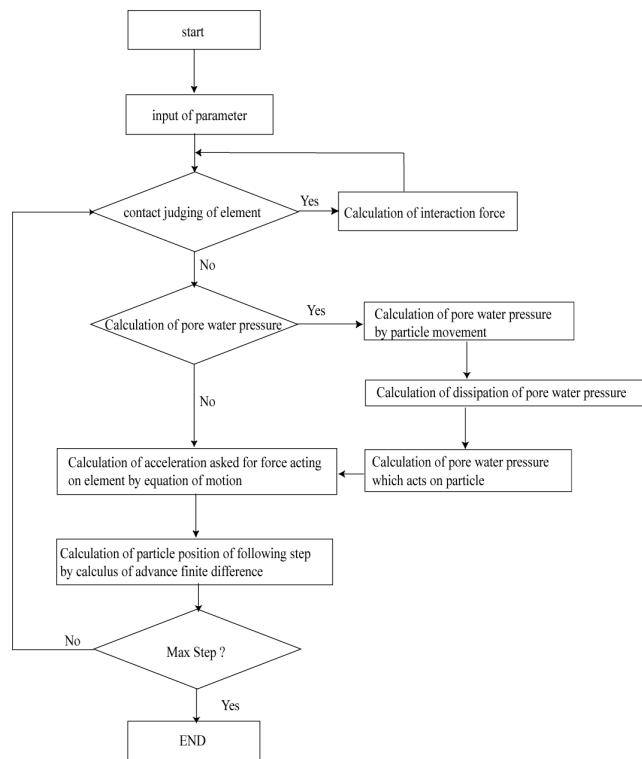


Figure 9: Flow of DEM

water pressure which acts on particle were repeated for every mesh.

DEM simulation of simple shear test of model ground

Analysis method

DEM analysis for the model test was performed by following the experimental procedures as closely as possible. First the construction of model ground was simulated by free falls of 4000 DEM elements into a shear box which has the same size of model test. The diameters of DEM elements were 7 times of actual silica sand, but the gradation properties such as the coefficient of uniformity was made similar to that of silica sand. It may be noted that PBD is modeled as a chain of DEM elements tightly connected together, and soil DEM elements are pulverized over PBD DEM model that is pre-installed in the box. After a steady state is achieved following the free falls, than the model ground was given a consolidation stress of 19.6 kPa. Then the horizontal loading was given at the top boundary of DEM model ground. The DEM elements at the top boundary were allowed to move only in horizontal direction without rotation nor vertical movements. When the shearing the shear box, a constant height condition was maintained by adjusting the vertical load on the model ground. In order to model the geo-grid effects, several DEM elements at the same level of PBD top and/or bottom ends were given the same horizontal movement of the PBD ends without rotations. The material properties for soil and PBD DEM elements are given Table 3. The same material constants are used for both the PBD and geo-grid, and these properties represent that of Type-2 PBD.

Analysis result

Table 3: Material properties of element and PBD elements

		Sand	PBD , Geo-grid net
Density	(kg/cm ³)	2640	1000
Normal spring coefficient	Kn (N/m)	2.00E+07	4.00E+08
Shear spring coefficient	Ks (N/m)	1.50E+07	3.00E+08
Normal damping coefficient	η_n (N · s/m)	5.20E+02	8.00E+02
Shear damping coefficient	η_s (N · s/m)	7.00E-03	8.00E+02
Cohesion	C (N)	0.0	
Friction angle	ϕ (degrees)	24.0	

The relationships between shear stress and shear strain are shown in Fig. 10 (a). The ground model without PBD shows the least resistance during the shear, and the resistance increases as the number of PBD installation increases. This trend of shear resistance increases with PBD installation agrees with the model experiments, but there are some inconsistencies in the analysis results with geo-grid installations. For the installations of two PBDs (i.e., DEM 1-1 & 1-2), the trend of DEM analysis is in agreement with the experimental result (i.e., the shear resistance is higher for the case of the base geo-grid installation compared with the case without the base geo-grid). However, for the installation of three PBDs (i.e., DEM 1-3 & 1-4), the

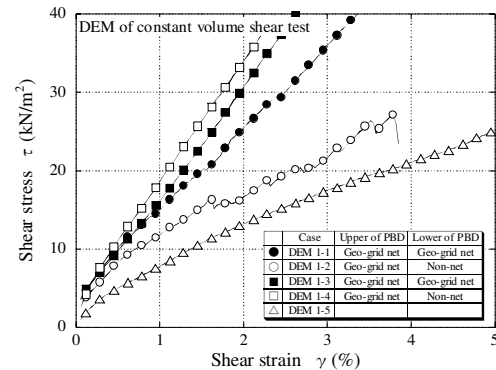


Figure 10(a): Shear stress - shear strain relationship

trend of DEM analysis is opposite to the experimental result. The reason for this discrepancy is examined later.

Fig. 10 (b) shows the relationship between vertical stress and shear strain. The analysis shows an almost similar trend with that of the experiment except for the result of the three PBDs installation. Fig. 10(c) shows the changes of effective stress during the shear, the analysis results are somewhat in mixed agreement with the experimental results. The model ground without PBD shows the largest reduction in effective stress during the initial shearing stage of test, and this agrees with the experiment.

However the increase of shear resistance with the increase of normal stress (the frictional resistance) of model ground is not in agreement with the experimental result. This aspect of analytical results can be further examined by plotting the distribution of contact forces among DEM soil elements. Fig. 11 shows the contact force distributions of DEM 1-1, 1-2, and 1-3 at shear strain of 3%. The figures clearly indicate the followings;

- a) The contact force distribution is not uniform within the model ground.
- b) The effect of PBD installation is to confine the soil particle movements within the space surrounded by PBD or the outer boundary of test apparatus.

For the model ground with PBD, there is a gradual change of soil state from the active earth pressure to the passive earth pressure states shown in the right to the left of Fig 11(1) respectively. On the other hand, the contact force distribution is distinctively different among the particles within three different spaces separated by the two PBDs in the model of Figs. 11(2), and (3). It is noted from the comparison of Figs 11(2) & (3), the model ground with base geo-grid installation induces more different concentrations of contact force within the confined spaces. This strongly confined zone of soil particles seems to develop a higher shear resistance and normal contact force. On the other hand, the normal stress plotted in Figs. 11 (a) & (b) is the average normal stress over the entire length of upper most boundary. Thus the non-uniformity of contact forces greatly influences the results shown in Figs. 11 (b) & (c). Also it is noted that the DEM analysis has 2-D limitations that prevents no particle movements across the vertical PBD walls, while in the actual experiments, the soil particle movements and PBD movements are relatively independent. These discrepancies between the

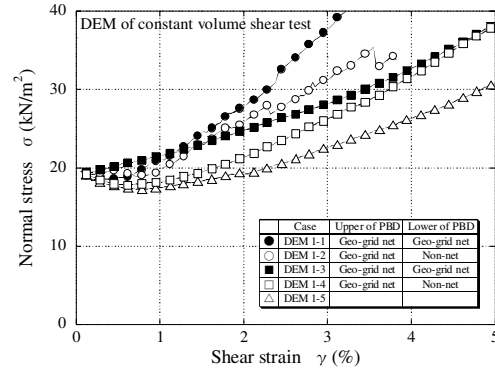


Figure 10(b): Normal stress - shear strain relationship

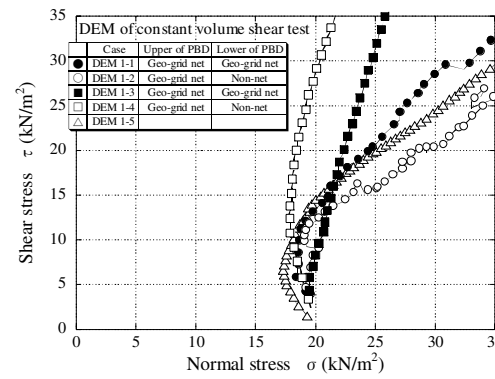


Figure 10(c): Effective stress path

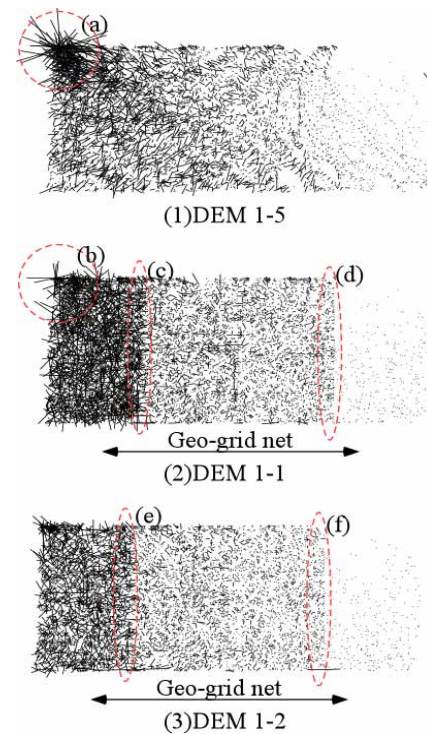


Figure 11: Contact force between elements ($\gamma = 3\%$)

experiment and DEM analysis may have resulted in the different trends of analysis results from the experiment. It is however most interesting to note that the PBD installation induce the spaces of particle confinements near PBDs, and, within these confinement spaces, higher particle contact forces are developed that seems to result in higher shear resistance of the ground.

The tensile forces developed in the PBD for different geo-grid installations are examined, and the depth distributions of these tensile forces are shown in Fig. 12. The PBD with the base geo-grid installation shows higher tensile forces along the PBD and the force distribution is not uniform with higher forces generated in the PBD near the base geo-grid.

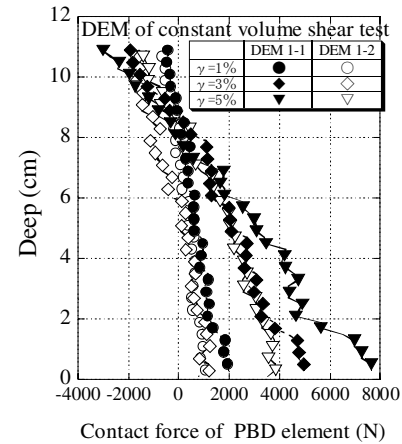


Figure 12: Contact force between PBD elements

Simulation analysis of monotoneous loading test

Analysis method

Here, in addition to the simulation analysis of a monotoneous loading test, the influence for the number of PBD, the stiffness of PBD, and the connection method to a geo-grid net is investigated.

The analysis model was created by the same method as the case of the simulation analysis of a constant volume shear test. The model is in a dryness state. Consolidation pressure is 39.6kPa. Analysis case is shown in Table 4. Example of analysis model is shown in Fig. 13. The installed interval of PBD was made into regular intervals. Left-hand side and right-hand side are the continuous periodic boundary. The element of the bottom end of PBD was made into rotation freedom. The size of model is length of 30cm, and height of 12cm. The material constant of element (sand), PBD, and a geo-grid net are shown in Table 5. The material constants of PBD are three cases.

Analysis carried out the shear of the bottom by the constant rate. While carrying out shear, the normal stress was made to fluctuate so that the height of traverse element may become fixed.

Table 4: Case of analysis (monotoneous loading test)

Case	Number of PBD	Type of PBD and geo-grid net(Parameter)	Upper of PBD
DEM 2-1	0		Non-geo-grid net
DEM 2-2	1	PBD-M	Non-geo-grid net
DEM 2-3	2		Geo-grid net
DEM 2-4	3		Geo-grid net
DEM 2-5	6		Geo-grid net
DEM 2-6	2	PBD-H	Geo-grid net
DEM 2-7	6		Geo-grid net
DEM 2-8	2	PBD-L	Geo-grid net
DEM 2-9	6		Geo-grid net
DEM 2-10	2	PBD-M	Non-geo-grid net
DEM 2-11	6		Non-geo-grid net

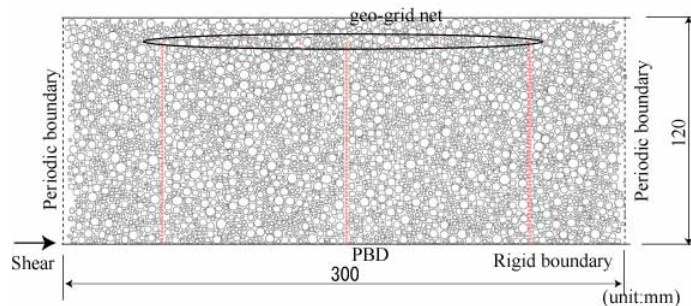


Figure 13: Example of DEM analysis model

Table 5: Material properties of element and PBD elements

		Sand	PBD , Geo-grid net		
			PBD-M	PBD-H	PBD-L
Density	(kg/cm ³)	2640	1000		
Normal spring coefficient	Kn (N/m)	4.00E+07	2.00E+08	4.00E+08	8.00E+07
Shear spring coefficient	Ks (N/m)	3.00E+07	1.50E+08	3.00E+08	6.00E+07
Normal damping coefficient	ηn (N · s/m)	2.60E+02	8.00E+02	8.00E+02	8.00E+02
Shear damping coefficient	ηs (N · s/m)	7.00E-03	8.00E+02	8.00E+02	8.00E+02
Cohesion	C (N)	0.0			
Friction angle	φ (degrees)	24.0			

Analysis result

The relationship between shear strain and shear stress is shown in Fig. 14(a). Except for DEM 2-2 connected the PBD top end by a geo-grid net, the shear stress becomes large, so that there are many installed numbers of PBD. The same result as a monotoneous loading test is shown.

The relationship between shear strain and normal stress is shown in Fig. 14(b). It is hard to compress and becomes easy to expand, so that the number of PBD increases.

The effective stress path is shown in Fig. 14(c). When PBD is 3 number, reduce of effective stress is the smallest. The test also shows the same tendency. According to DEM, it is thought that there is optimal number in reinforce of ground.

Next, influence for the stiffness of PBD or the difference of the connection method with a geo-grid net is described.

(1) The stiffness of PBD (Fig. 14(d))

Reduce of effective stress becomes large, so that the stiffness of PBD is large. However, the shear stress will become large if it passes over a phase transformation.

(2) The connection method of PBD and geo-grid net (Fig. 14(e))

When the case connected PBD top end by a geo-grid net, reduce of the effective stress is smaller than the

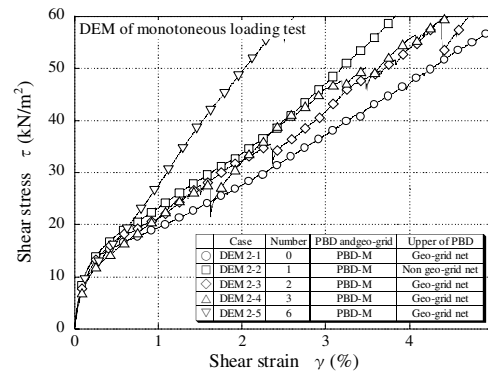


Figure 14(a): Shear stress - shear strain relationship

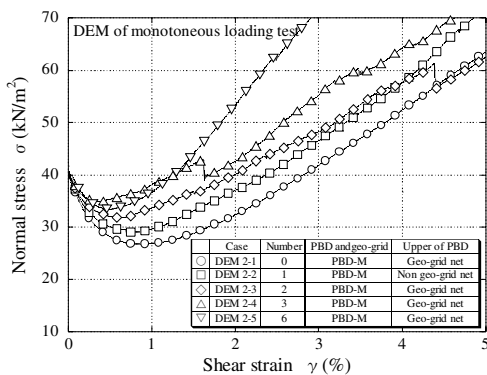


Figure 14(b): Normal stress - shear strain relationship

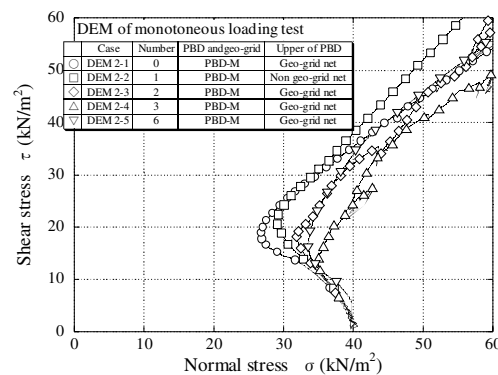


Figure 14(c): Effective stress path

case where it does not connect. The shear stress will also become large if it passes over a phase transformation.

The contact stress distribution for every PBD elements is shown in Fig. 15(a) - (d). The value of the X-axis is tension stress per PBD.

Fig. 15(a) (b) expresses the contact stress distribution in case PBD are 2 numbers, 3 numbers, and 6

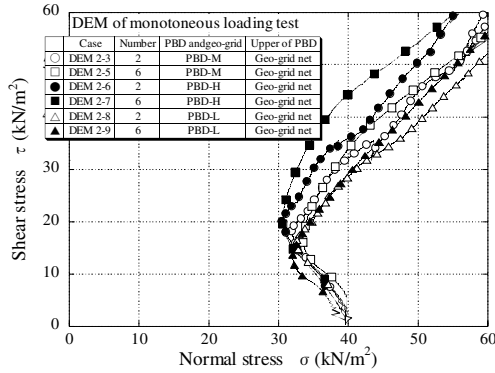


Figure 14(d): Effective stress path

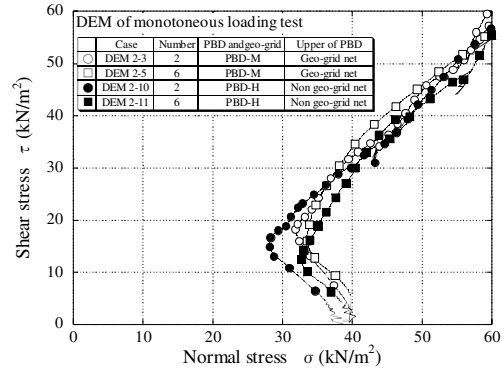


Figure 14(e): Effective stress path

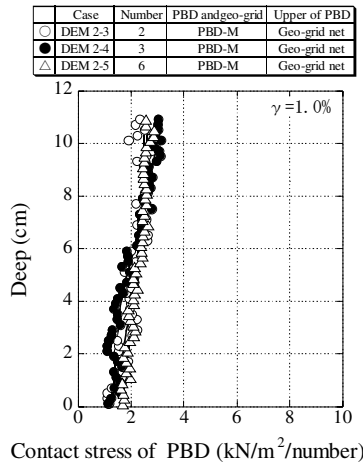


Figure 15(a): Contact stress of PBD($\gamma = 1.0\%$)

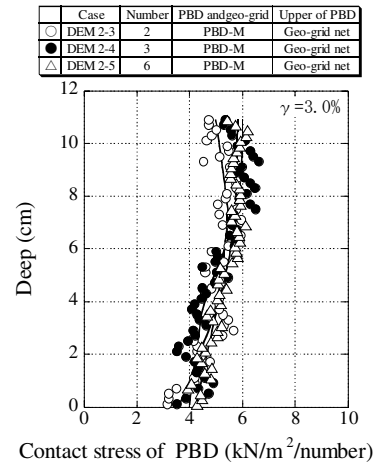


Figure 15(b): Contact stress of PBD($\gamma = 3.0\%$)

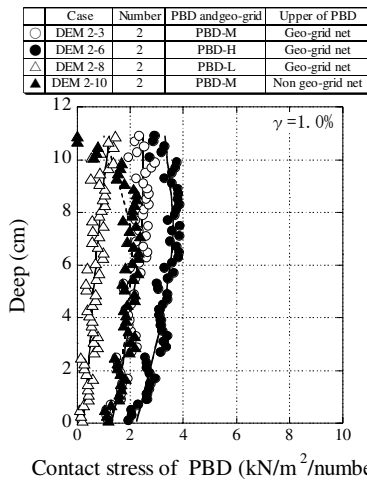


Figure 15(c): Contact stress of PBD($\gamma = 1.0\%$)

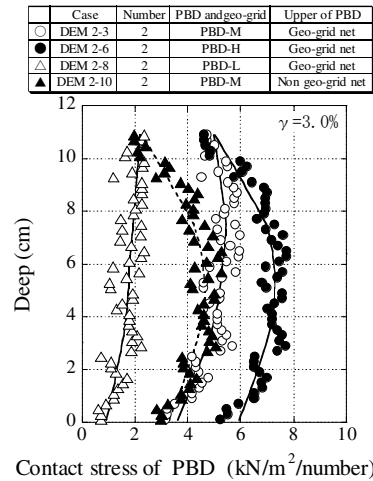


Figure 15(d): Contact stress of PBD($\gamma = 3.0\%$)

numbers. Irrespective of the number of PBD, the tension stress per one is almost the same. The value will become large if shear strain becomes large. Moreover, the value near the PBD upper part is large under the influence of a geo-grid net. Fig. 15(c) (d) is figure about the contact stress distribution at the time of changing the stiffness of PBD. Tension stress becomes so large that the stiffness of PBD is large. The value near the PBD upper part of DEM 2-10 without a geo-grid net is very low. It differs from DEM 2-3 with a geo-grid net. The confining effect is exerted by connecting PBD with a geo-grid net.

CONCLUSION

This research performs a laboratory test of the specimen installed PBD and simulation analysis used DEM of the model installed PBD, and the drainage effect of PBD and the confining effect of the ground installed PBD and a geo-grid net are examined.

The result of a laboratory test in ground installed PBD showed the following things.

- (1) The shear stiffness of ground becomes large by PBD with a geo-grid net. Moreover, the shear stress becomes so large that the number of PBD increases.
- (2) On the ground installed PBD, reduce of effective stress is small. (The ground installed PBD will be hard to liquefaction easily.)
- (3) The confining effect of ground is exerted by the tension of PBD. Furthermore, the effect increases by PBD with a geo-grid net.
- (4) A laboratory test was also able to check the reinforce effect of PBD in a shaking table test.

The result of the simulation analysis using DEM showed the following things.

- (1) The result of a laboratory test was reproducible although it was qualitative.
- (2) The confining effect of the ground changes with the number of PBD, the stiffness of PBD, and connection methods with a geo-grid net.
- (3) When PBD vertical end was connected by a geo-grid net, the contact force between elements of the domain surrounded by PBD is almost uniform. It seems that the action of PBD and ground element unified (winning by PBD and a geo-grid net).
- (4) The force acts on the connection part of PBD and a geo-grid net.

From now on, it is considered that the synergistic effect which considered the drainage characteristic of PBD and confining effect of PBD with a geo-grid net.

ACKNOWLEDGEMENT

The program improved "DEMS" which Sumio Sawada (Kyoto University) developed was used for this analysis. I describe and appreciate.

REFERENCES

1. Y Mizoguchi, T Aasada, Y Tanaka. "the liquefaction characteristic of plastic board drain installed ground", The 11th Japan Earthquake Engineering Symposium, pp721- 726, 2002
2. Y Tanaka, T Nishigata, Y Mizoguchi. "The shear property of plastic board drain installed ground by a simple shear test", 57th meeting of Japan Society of Civil Engineers, the CD-ROM version, 2002
3. Cundall and P.A. "A Computer Model for Simulating Progressive Large Scale Movement in Blocky Rocksystem", Symposium ISRM, Proc.2, and pp.129- 136 and 1971
4. M Fijitani, H Ishikawa, H Nakase, H Mogi. "The simulation of the liquefaction used the distinct element method", 24th JSCE Symposium on Earthquake Engineering, pp.489- 492, 1996
5. H Nakase. "Application of the distinct element method to the liquefaction of ground", Proceeding of the 33th Japan national conference on geotechnical engineering, pp.975- 976, 1998

6. H Nakase, A Honda, T Nishino, "A numerical study of establishment of friction parameters for DEM analysis", Proceeding of the 36th Japan national conference on geotechnical engineering, pp.503- 504 , 2001